

# RGD Peptide-Functionalized Polyether Ether Ketone Surface Improves Biocompatibility and Cell Response

Lillian V. Tapia-Lopez, María A. Luna-Velasco, Elfa K. Beaven, Alain S. Conejo-Dávila, Md Nurunnabi, and Javier S. Castro\*



Cite This: <https://doi.org/10.1021/acsbomaterials.3c00232>



Read Online

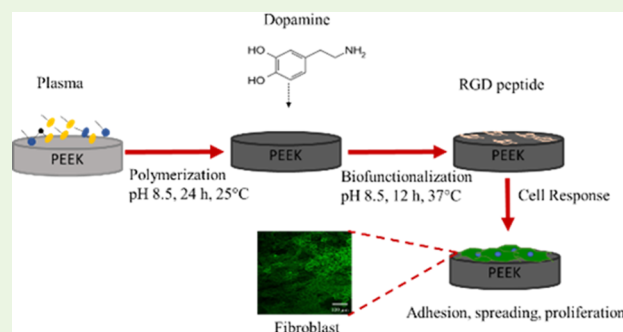
ACCESS |

Metrics & More

Article Recommendations

**ABSTRACT:** Polyether ether ketone (PEEK) is a biocompatible polymer used in maxillofacial and orthopedic applications because of its mechanical properties and chemical stability. However, this biomaterial is inert and requires surface modification to make it bioactive, enhancing implant-tissue integration and giving the material the ability to interact with the surrounding microenvironment. In this paper, surface of PEEK was activated by oxygen plasma treatment and this resulted in increasing reactivity and surface hydrophilicity. Then, a polydopamine (PDA) coating was deposited over the surface followed by biofunctionalization with an RGD peptide. The plasma effect was studied by contact angle measurements and scanning electron microscopy. X-ray photoelectron spectroscopy confirmed the presence of PDA coating and RGD peptide. Crystallinity and phase identification were carried out through X-ray diffraction. Quantification of the immobilized peptide over the PEEK surface was reached through UV-vis spectroscopy. In addition, *in vitro* tests with fibroblast cell line (NIH/3T3) determined the viability, attachment, spreading, and proliferation of these cells over the modified PEEK surfaces. According to the results, PEEK surfaces functionalized with peptides demonstrated an increased cellular response with each successive surface modification.

**KEYWORDS:** peptide coating, functionalization, bioactivity, surface modification, polymer/PEEK



## 1. INTRODUCTION

The advancement of implantable bioactive materials in the medical field has improved the quality of life for many patients.<sup>1</sup> Bioactive materials must generate a positive response to the host biological environment creating a suitable implant-tissue integration while avoiding the formation of surrounding fibrous tissue, toxicity, infection, activation of the immune system, and consequently, in short or long term, implant rejection.<sup>2</sup> Due to the importance of using bioactive biomaterials for implants, several studies have been carried out on surface modification to create bioactive surfaces with adequate protein adsorption, cellular response, and tissue integration.<sup>1,3,4</sup> With surface chemistry and a hydrophilic surface, proteins can be adsorbed to the surface of biomaterials favoring an orientation that promotes cell migration, adhesion, and spreading.<sup>3,5–7</sup> In the present work, we are proposing the biofunctionalization of the polyether ether ketone (PEEK) surface with polydopamine (PDA) and the GRGDSP fibronectin-sequence peptide to increase bioactivity and improve the implant–tissue interaction. We establish a new way to transform inert biomaterials into bioactive ones to improve the interaction implants have with living tissues for superior incorporation and sustainable long-term results.

Herein, we propose a novel method to functionalize the surface of PEEK to enhance tissue–implant interactions. PEEK was chosen because it is a plastic polymer used as bone substitute in orthopedics and craniofacial and spine reconstruction surgeries due to its chemical stability<sup>4</sup> and suitable mechanical properties; it presents aromatic rings and carbonyl functional groups in the polymer main chain that provide a semicrystalline structure making it a hard, durable, hydrophobic, and unreactive material.<sup>4,8</sup> PEEK also has a smaller elastic modulus than cortical bone which avoids stress shielding. Furthermore, it has worn resistance, radiolucency, low density, is non-allergenic, non-corrosive, non-toxic, and non-mutagenic.<sup>9,10</sup> All these features make it an excellent material to be implanted in the human body however because PEEK is a bioinert polymeric material, different methods have been used to modify its surface characteristics to make the

Received: February 22, 2023

Accepted: August 4, 2023

molecule bioactive.<sup>5,6,11,12</sup> In this work, the PEEK surface was activated with oxygen plasma and coated with PDA, following a biofunctionalization with an GRGDSP fibronectin peptide; the RGD sequence is reported as an activator of integrin transmembrane cells.<sup>13–16</sup>

Briefly, our process consisted of PEEK surface polishing to remove any marks from the cutting process and a treatment with oxygen plasma as primer activation by introduction of oxygen-functional groups to enhance the adhesiveness<sup>11</sup> and hydrophilicity of the surface.<sup>7,12</sup> Then, the surface was rinsed with DI water to stabilize it and remove any low-molecular-weight debris possibly generated by plasma.<sup>3,17</sup> The subsequent surface modification involved PDA coating under alkaline conditions to perform an oxidative polymerization reaction over PEEK.<sup>11,18,19</sup> Dopamine is a catechol amine compound used to coat different surfaces such as polymers, ceramics, and metals<sup>5,18</sup> and has functional groups that facilitate the attachment of biomolecules like peptides, proteins, and growth factors, as reported previously.<sup>5,13</sup> Due to the surface modification with PDA coating, the attachment of the bioactive and functional peptide GRGDSP was achieved. The peptide contains the sequence Arg-Gly-Asp, recognized by integrin proteins found in the cell membrane.<sup>13,14,16</sup> The objective of working with a peptide instead of a protein is that it offers a low risk of immunological reactivity. In addition, being a small peptide presents stability to sterilization, pH variation, and temperature<sup>15</sup> as well as higher integrin affinity.<sup>16</sup> These modifications aim to improve the bioactivity in vitro related to migration, adhesion, spreading, and proliferation of fibroblast cells on the modified surfaces.

## 2. EXPERIMENTAL SECTION

**2.1. Materials.** Dental PEEK was purchased from Cera Direct (China). Dopamine hydrochloride, Tris (hydroxymethyl) aminomethane buffer, and Dulbecco's modified essential medium (DMEM-F12) were purchased from Sigma-Aldrich (USA). Fetal bovine serum (FBS) was acquired from Gibco. GRGDSP peptide fibronectin derived was purchased from GenScript (USA). NIH/3T3 mouse fibroblast cells were acquired from ATCC (CRL-1658). Hoechst 33342 was purchased from Abcam (USA) and Phalloidin CF488A from Biotium (USA).

**2.2. Sample Preparation.** **2.2.1. Design and Polishing.** First, PEEK disc samples with a height of 3 mm and different diameters, 18 mm for contact angle measurements, 5.8 mm for cell viability assays, and 10 mm for all other assessments, were designed in Solid Works® software and milled in a dental milling machine, Roland DWX-51D (Hamamatsu, Japan). The samples were then randomly polished with aluminum oxide sandpapers, using different grits (320, 600, 1200, and 2000) for 20 s each in a micro rotator GPX 200 Leco. Finally, they were sonicated in ethanol and DI water to remove any residues from the polishing process for 30 and 5 min, respectively. A polished sample without additional surface treatment was considered as a control sample and named polished-PEEK (PP), as shown in Table 1.

**2.2.2. Plasma Surface Treatment.** PP samples were oxygen plasma treated for surface activation<sup>7,20</sup> using a low-pressure plasma system from the Diener Plasma Technology model Femto Standard Version (Germany) to create PP treated with oxygen plasma (PLP). The gas

entered inside the chamber at a 5 ssc flow rate, 0.5 mbar pressure, power 50 W, vacuum pump speed 1.5 m<sup>3</sup>/h, and generator frequency 40 kHz for 1 min. Samples were thoroughly rinsed with DI water twice for plasma stabilization over the surface and eliminate the possible low-molecular-weight debris produced during the gas discharge, reducing the surface concentration of oxygen.<sup>3,7,17</sup> A strategy to modify the PEEK surface consists of irradiating it with plasma varying mainly in intensity and irradiation time. Exposition to high energy produces the fragmentation of the PEEK main chain in ether bonds and carbonyl functional groups. Also, oxygen plasma introduces new functional groups derived from oxygen, such as alcohols, carboxylic acid, and aldehydes. The reduction of polymer size and the presence of functional groups with oxygen reduce the material's hydrophobicity, providing reactive sites for interactions with other elements or molecules.<sup>11,21</sup>

**2.2.3. Polydopamine Coating.** PLP samples were immersed in a solution of dopamine hydrochloride (2 mg/mL) in Tris buffer (10 mM, pH 8.5) at room temperature<sup>22</sup> and constantly stirred for 12 h. Then, samples were rinsed with DI water using an orbital shaker at 100 RPM for 10 s to remove any unbonded dopamine;<sup>7</sup> this was repeated twice.<sup>5</sup> Finally, the samples were sterilized with ethanol, dried under a laminar flow chamber, and stored in a desiccator, thus creating the plasma-PEEK coated with PDA (DPP). The polymerization mechanism of PDA is not currently clarified; nevertheless, various research studies agree that the polymerization process starts with the oxidation of dopamine to produce quinoid derivatives;<sup>6,13,18</sup> once in this structure, the mechanism could take three different routes. The first one involves the propagation process using the quinoid dopamine structure as a monomer where the reactive sites are carbon 3 and 5. The second mechanism uses a cyclization reaction of quinoid dopamine through an aza-Michael intermolecular response to produce the 5,6-dihydroxyindole (DHI). The reactive sites for oxidative propagation are carbon 2 and 4. The third route of oxidative polymerization consists of a mix of the previous two, with quinoid dopamine and DHI reacting through an oxidative reaction in their respective reactive sites. It is worth noting that in all cases of the abovementioned polymerization mechanisms, alcohol functional groups use it as a substituent in the polymer main chain. These functional groups act as reactive sites to produce hydrogen bridge bonds or electrostatic interactions with other compounds.<sup>18</sup>

**2.2.4. RGD Immobilization.** The final sample preparation of dopamine-PEEK functionalized with peptides (PEP) for RGD immobilization was made using the DPP samples. Samples were incubated with the peptide solution, fibronectin sequence: GRGDSP (Gly-Arg-Gly-Asp-Ser-Pro) 500 µg/ml (0.85 mM) in Tris buffer (10 mM, pH 8.5) for 12 h at 37 °C.<sup>23</sup> Afterward, samples were twice rinsed with PBS buffer to remove unattached peptides that may cause cell detachment.<sup>14</sup> The binding between the peptide and PDA coating (speculated to have mainly OH groups)<sup>5,18,23</sup> is through electrostatic interactions between the coating and the hexapeptide.

**2.3. Surface Characterization.** **2.3.1. Surface Hydrophilicity.** The static contact angles were measured at room temperature for all samples using the FTA-200 equipment. Measurements were made approximately 20 min after each surface treatment. A 2 µL drop of distilled water was automatically deposited on the surface of the samples using a surgical syringe with a precision flow control valve. Measurements were automated using FTA image analysis software. For each sample, six contact angles were measured and averaged. Standard deviations ranged from 2.08 to 5.34°.

**2.3.2. Surface Topography.** The surface topography of the samples was analyzed by scanning electron microscopy (SEM) using a JEOL 7401 JSM microscope. Magnification: 10 kX, acceleration voltage 3 kV, probe current 9 to 10 µA, and field emission electron gun (tungsten tip emitter) under ultra-high vacuum.

**2.3.3. Quantification of Immobilized RGD Peptide.** Immobilized RGD peptide over DPP samples was quantified by evaluating the peptide concentration in the solution before and after the biofunctionalization process and doing a mass balance. In brief, the initial peptide concentration in the solution is well known. Then, after PEEK treatment, the sample was thoroughly rinsed, and the

**Table 1. Sample Preparation and Their Naming**

sample name	surface modification
PP	polished-PEEK
PLP	polished-PEEK treated with oxygen plasma
DPP	plasma-PEEK coated with polydopamine
PEP	dopamine-PEEK functionalized with peptides

absorbance of peptide in the retrieved solution was measured using UV–visible spectroscopy. The experiment was performed in duplicate.

The peptide concentration in the solution was calculated by interpolating the absorbance of the mean of the samples with a previously prepared calibration curve using GraphPad Prism software.

Thus, the peptide masses in the solution before and after PEEK surface treatment were calculated. The RGD peptide concentration in the solution was quantified using UV–visible spectroscopy (Cary 5000, Agilent) at 200–350 nm wavelength. It is stated that the maximum signal is detected near 190 nm ( $\pi \rightarrow \pi^*$ ) and the minimum at 220 nm ( $n \rightarrow \pi^*$ ).<sup>24</sup>

**2.3.4. Chemical Composition.** X-ray photoelectron spectroscopy (XPS) was used to determine the elements present on all surfaces, using a Thermo Scientific Escalab 250xi instrument equipped with an Al K $\alpha$  monochromatic X-ray source ( $h\nu = 1486.86$  eV) and 0.4 resolution,  $-0.6$  eV. The voltage applied to the electron gun was 10 eV, spot size 650  $\mu\text{m}$ , energy step size 1.00 eV, using a standard lens, and step energy 200 eV. All samples were measured 48 h after each surface modification.

**2.3.5. X-ray Diffraction-Phase Identification.** Since PEEK and peptide show some degree of crystallinity, X-ray diffraction (XRD) analysis was conducted to phase identification of each sample to detect the presence of peptide on the surface. The analysis used a PANalytical XpertPRO diffractometer with a Cu-K $\alpha$  radiation source, operated at 40 kV and 30 mA. The diffractograms were recorded from  $2\Theta$ , the angle range of  $7-90^\circ$ , with a step size of  $0.013^\circ$ .

**2.4. Cellular Response.** **2.4.1. Cell Culture.** NIH/3T3 mouse fibroblasts (ATCC, CRL-1658) were cultured in Dulbecco's modified essential medium (DMEM-F12), supplemented with 5% FBS and 1% streptomycin. Cells were incubated at  $37^\circ\text{C}$  and 5%  $\text{CO}_2$ . The cells were passaged every 2–3 days and detached using 0.25% Trypsin–EDTA solution (Sigma-Aldrich).

**2.4.2. Cell Viability (MTT Assays).** Cell viability was determined using a colorimetric 3-(4,5-dimethylthiazol-2-yl)-2,5-diphenyltetrazolium bromide (MTT) assay to measure cellular metabolic activity. Living cells reduced MTT to a purple formazan salt, a measurable marker.<sup>15,25</sup> Each PEEK sample was placed in a 96-well plate, in triplicate, and NIH/3T3 fibroblasts were seeded on the surface of the PEEK sample discs at a density of  $2 \times 10^4$  cells/well with DMEM-F12 medium supplemented with 5% FBS. For the control, NIH/3T3 fibroblasts were seeded in triplicate on a 96-well plate at a final volume of 200  $\mu\text{L}$  per well. The plates were incubated at  $37^\circ\text{C}$ , 5%  $\text{CO}_2$ , and 92% humidity for 1, 3, and 5 days.

Following each day, the medium of each well was aspirated, and cells were washed with PBS. DMEM-F12 and MTT stock solution (0.5 mg/mL) were added to each well, and the plates were incubated for another 4 h at  $37^\circ\text{C}$ . After 4 h, the MTT with the medium was removed from each well, and dimethyl sulfoxide was added for about 10 min to solubilize the formazan crystals generated by the cell's mitochondrial activity. Then, 100  $\mu\text{L}$  of solubilized formazan crystals was transferred to a 96-well plate, and the absorbance was read at 570 nm in a microplate reader Varioskan Lux VLBLATD2, Thermo Fisher Scientific (Massachusetts, USA). Cell viability in the samples was calculated as a percentage of the optical density, considering the optical density of the control represented 100% viability. All assays were made by duplicate.

$$\% \text{ Viability} = \left( \frac{\text{optical density sample}}{\text{optical density control}} \right) \times 100$$

**2.4.3. Cell Proliferation.** PEEK samples were placed in a 24-well plate, and fibroblasts were seeded onto each surface at a density of  $2 \times 10^4$  cells using DMEM-F12 medium supplemented with 5% FBS at a final volume of 1 mL per well. They were incubated at  $37^\circ\text{C}$ , 5%  $\text{CO}_2$ , and 92% humidity for 1 and 5 days. Following incubation time, each surface was rinsed with PBS, and the cells' nuclei were stained according to a protocol described previously.<sup>26</sup> Briefly, cells were washed with PBS and fixed with 3.75% paraformaldehyde for 15 min at  $4^\circ\text{C}$ . Subsequently, a permeabilization process was carried out with

triton X-100 at 0.2% for 10 min at room temperature. Hoechst fluorochrome was used to stain the cells' nuclei at  $37^\circ\text{C}$  for 30 min. To observe the cell proliferation, cell counting was performed. Sample images were taken at the first and fifth day. At least 20 images per sample were taken for each sample group ( $n = 2$ ). From the images obtained at 10 $\times$  magnification, the cell count per area was performed using Image J software.

**2.4.4. Cell Attachment and Spreading.** PEEK sample discs were placed in a 24-well plate, and fibroblasts were seeded onto each surface at a density of  $2 \times 10^4$  cells using DMEM-F12 medium supplemented with 5% FBS at a final volume of 1 mL per well. They were incubated at  $37^\circ\text{C}$ , 5%  $\text{CO}_2$ , and 92% humidity for 1 and 5 days. This step allowed the cells to adhere and proliferate on the surface of the samples. The samples were rinsed with PBS, and the cytoskeleton was stained according to a protocol described previously.<sup>26</sup> Briefly, cells were washed with PBS and fixed with 3.75% paraformaldehyde for 15 min at  $4^\circ\text{C}$ . Subsequently, a permeabilization process was carried out with triton X-100 at 0.2% for 10 min at room temperature followed by blocking with lactose protein (10% in PBS; 1 h) at room temperature. Phalloidin fluorochrome was used to stain the actin filaments for 20 min at room temperature in the absence of light followed by three washes with PBS. Finally, the samples were analyzed using a confocal microscope (Zeiss LSM-700). The cell morphology was studied with SEM, and cells were seeded on peek samples at a density of  $2 \times 10^4$  cells and incubated at  $37^\circ\text{C}$ , 5%  $\text{CO}_2$ , and 92% humidity for 8 h. Then, cells were fixed with 2.5% glutaraldehyde followed by 8 h in a refrigerator at  $4^\circ\text{C}$ . After washing them with PBS, the cells were dehydrated, and samples were soaked in different ethanol and DI solutions (20, 30, 50, 70, 90, 95, and 100%) for 5 min each. After that, the samples were dried, and gold sputtered. The images were analyzed using a Hitachi SU3500 (magnification 5.00 and 3.00 $\times$ , acceleration voltage 5 kV, and working distance of 6.2 mm).

**2.5. Statistical Analysis.** Quantitative data are expressed as mean  $\pm$  standard deviation (SD as error bars). Statistical significance was performed with the analysis of variance Brown-Forsythe and Welch's ANOVA and Dunnett's T3 test using GraphPad Prism software. A value of  $p < 0.05$  was considered statistically significant.

### 3. RESULTS AND DISCUSSION

**3.1. Surface Hydrophilicity.** Average contact angle measurements are presented for the different PEEK surfaces in Figure 1. The contact angle after each treatment of surface modification is smaller than the previous one. The smaller the

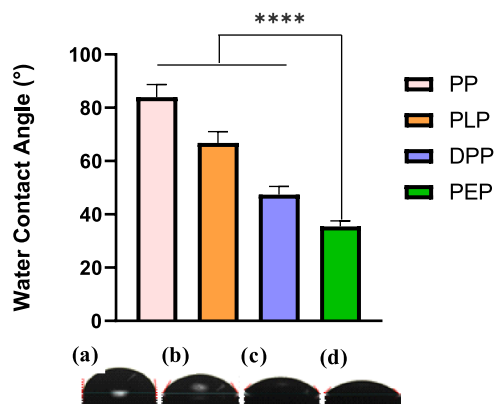


**Figure 1.** Measurements of water contact angle and representative pictures of water droplets on PEEK samples, (a) PP, (b) PLP, (c) DPP, and (d) PEP. Data were obtained from five independent measurements ( $n = 5$ ); \*\*\*\* represents  $p < 0.0001$  compared to the PEP group, indicating a significant change in the contact angle values. The lower the water contact angle, the higher the surface wettability. The bars represent the standard error.

contact angle, the more hydrophilic the surface of PEEK is allowing the water droplet to spread out on the surface of the sample. As the contact angle decreased, the surface energy increased, establishing that each subsequent surface modification treatment increased the surface hydrophilicity.

The PP sample had the highest contact angle ( $83.9 \pm 5.34^\circ$ ), Figure 1a. The plasma treatment increased the PEEK surface hydrophilicity, thus decreasing the contact angle ( $66.8 \pm 4.11^\circ$ ) due to introduction of oxygen functional groups from modifying the surface with oxygen plasma,<sup>7,20</sup> Figure 1b. It is worth mentioning that this contact angle was due not only to the plasma treatment since this treatment would give a much lower value but also to the washing after the treatment because it reduces the oxygen content and stabilizes the effect of plasma.<sup>3,7,17</sup> As shown in Figure 1c, the contact angle for PEEK modified with PDA of  $47.4 \pm 3.67^\circ$  is due to the polar functional groups (OH) exposed on its surface.<sup>23</sup> Finally, the peptide also contains polar functional groups<sup>10</sup> that made the PEP sample the most hydrophilic with a contact angle of  $35.5 \pm 2.08^\circ$ , Figure 1d. The addition of the OH groups increases the ability of the surface to hydrogen bond with the water droplet which is why the water droplets can spread more over the surface of the PEEK discs after each successive treatment.

**3.2. Surface Topography.** Differences in topography of SEM images taken of PEEK surfaces are observed in Figure 2.

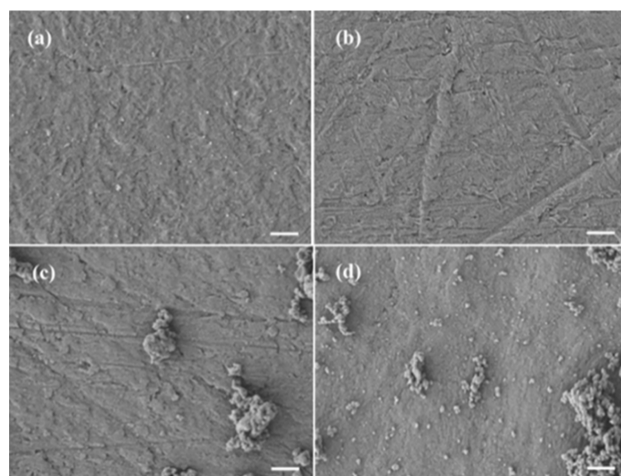


**Figure 2.** SEM surface characterization of PEEK samples to examine topography, (a) PP, unmodified PEEK, (b) PLP, O<sub>2</sub> plasma treated, (c) DPP, PDA-coated, and (d) PEP, functionalized with RGD peptide. Scale bars 1  $\mu\text{m}$ .

As shown in Figure 2a of the PP sample, any observable polishing mark does not appear. The PLP-treated sample shows a slight smoothing effect due to the oxygen plasma surface modification. The sample modified with the PDA coating (DPP) shows residues most likely due to dopamine polymerization, and the PEP sample also showed slightly different residues with a higher concentration than the DPP, Figure 2c,d, respectively.

**3.3. Quantification of the RGD Peptide.** Based on UV-visible spectroscopy analysis, GRGDSP peptide showed an absorbance at 208 nm wavelength, Figure 3. GRGDSP concentration was calculated as  $7.3 \mu\text{g/mL}$  according to the calibrated curve, then the mass was obtained as  $21.7 \mu\text{g}$ . Thus, the total amount of peptide over the surface is  $3.3 \mu\text{g}$ , which

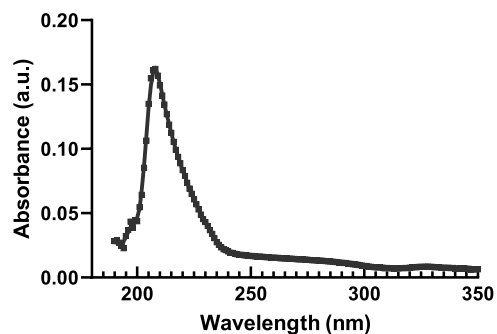


**Figure 3.** UV-vis absorption spectra for RGD peptide in the retrieved solution.

means that  $4.29 \times 10^{13}$  peptide molecules per  $\text{mm}^2$  are present in a surface of  $78.54 \text{ mm}^2$ .

**3.4. Chemical Composition.** **3.4.1. Polydopamine Coating and RGD Immobilization.** The XPS atomic percentage composition revealed that the C 1s and O 1s of PP and PLP is almost the same, likely due to the fact the PLP sample was rinsed after plasma treatment which reduces the surface oxygen concentration.<sup>7</sup> After PDA coating of the DPP sample, N 1s atomic percentage was detected due to the polymerization carried out. N 1s content also increased after peptide biofunctionalization of the PEP sample because of the higher content of amine groups shown in Table 2. These results were

**Table 2. Atomic Percentage Composition Detected on PEEK Surfaces**

samples	C 1 s	O 1 s	N 1 s
PP	$79.7 \pm 0.28$	$20.3 \pm 0.2$	
PLP	$78.9 \pm 0.33$	$21.1 \pm 0.33$	
DPP	$73.4 \pm 0.08$	$21.9 \pm 0.45$	$4.8 \pm 0.37$
PEP	$71.4 \pm 0.96$	$21.1 \pm 0.64$	$7.5 \pm 0.33$

related with the XPS survey spectrum and high-resolution spectra seen in Figure 4a. PP and PLP samples displayed only C 1s and O 1s peaks around 289 eV and 537 eV, respectively. In the DPP and PEP samples, the appearance of the N1s peak around 400 eV confirmed the PDA coating and the presence of the peptide. Furthermore, the modified PEEK surface high-resolution spectra were analyzed using NIST XPS database observed in Figure 4b. For N 1s peak of the DPP sample, the signal was deconvoluted into two curves, and N-H/NH<sub>2</sub> were detected, confirming successful modification of the PDA coating. After the peptide biofunctionalization, two curves were also obtained, and the NH<sub>2</sub> signal was detected in both, confirming the amine groups from amino acids of the RGD peptide sequence.

High-resolution spectra were obtained for the C 1s peak. For all samples, C=O/C-O/C-H binding energies were detected. In addition, for the PDA coating on the DPP sample, C-OH/C-N signals were demonstrated. The C-N signal was also detected for the PEP sample. The XPS results demonstrate the PDA coating and the biofunctionalization with the RGD peptide sequence were successful.

**3.5. XRD Phase Identification.** Figure 5a shows the X-ray diffractogram obtained for each PEEK sample. As it was expected, all XRD patterns showed the orthorhombic crystalline structure of PEEK observed at  $2\theta$  values of  $18.81$ ,  $20.78$ ,  $22.75$ , and  $28.77^\circ$  corresponding to the crystallographic

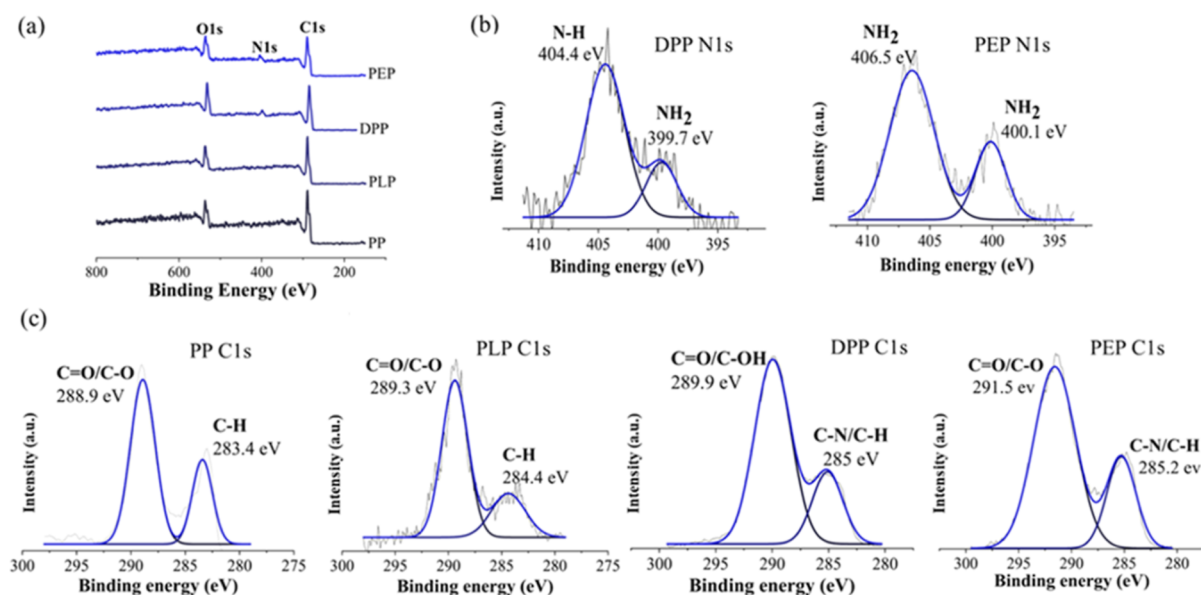


**Figure 4.** XPS surface chemical analysis, (a) survey spectrum of the different peek surfaces and the high-resolution spectra of (b) N 1s peaks for DPP and PEP samples, and (c) C 1s peaks detected in all samples, PP, PLP, DPP, and PEP.

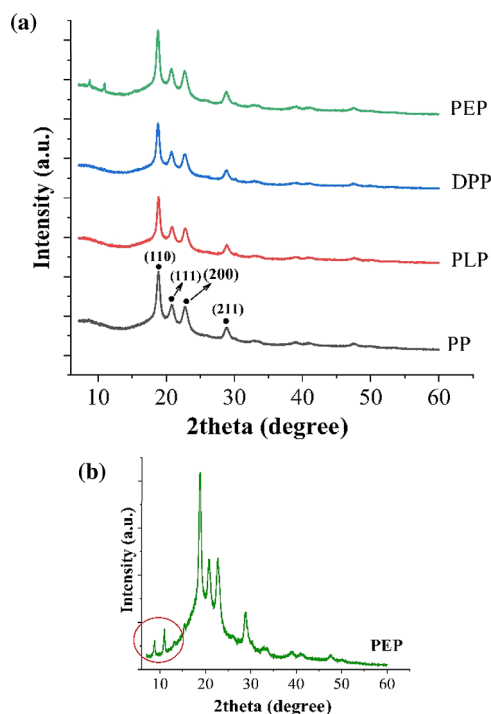


**Figure 5.** XRD patterns for phase identification in PEEK samples. (a) Samples: PP, PLP, DPP, PEP, and (b) grazing-incidence XRD pattern for the PEP sample to confirm peptide presence.

planes (110), (111), (200), and (211), respectively, and the amorphous phase observed as a hump at the low  $2\theta$  angles as has been reported previously.<sup>27,28</sup> The  $O_2$  plasma treatment and the PDA amorphous layer over surface PEEK, PLP, and DPP samples, did not show anything on the XRD pattern. Nevertheless, the PEP sample containing the RGD peptide showed two peaks at  $8.74^\circ$  and  $10.89^\circ$ . These peaks unequivocally belong to a different phase besides PEEK, and it must be a material with some degree of crystallinity, as could be an organic peptide,<sup>29,30</sup> such as the RGD peptide. Also, their low intensity demonstrates the small amount of that

phase compared to the substrate. In addition, to reinforce the previous finding, another PEP sample was also analyzed with grazing-incidence XRD (Figure 5b). This technique is commonly used for thin-layer analysis since the beam does not penetrate deep into the bulk but over the surface. Here, the two peaks observed previously were more visible and taller since the grazing-incidence beam improves the detection of thin layers over surfaces. Therefore, these peaks could be a reliable indicator of the peptide's presence over the surface. However, a thorough and more specialized analysis may be necessary to ensure it, which escapes from the aim of this work.

**3.6. Cellular Response.** **3.6.1. Cell Viability (MTT Assays).** The cell viability was analyzed in all PEEK samples (PP, PLP, DPP, and PEP) on the first, third, and fifth day which is represented in Figure 6.

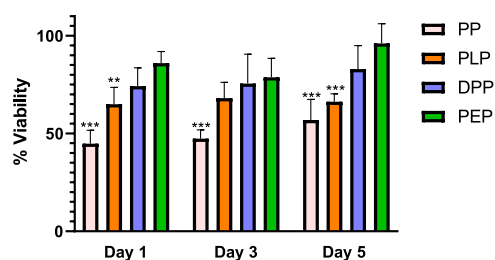


**Figure 6.** MTT assay to determine Fibroblast NIH /3T3 cell viability for the different PEEK samples, PP, PLP, DPP, and PEP. Measurements were taken on the first, third, and fifth days and estimated (based on a positive control), ( $n = 6$ ); \*\*\* represents  $p < 0.0001$ , and \*\* represents  $p < 0.001$  compared to the PEP group.

With each subsequent surface modification, there are more live cells as seen in Figure 6. Day 1 shows that the PP surface had a viability of  $45\% (\pm 3.92)$ , PLP  $65\% (\pm 1.74)$ , and DPP  $74\% (\pm 1.37)$  while for the PEP surface, the viability was  $86\% (\pm 4.42)$ . The trend of increased cell viability is similar on days 3 and 5. The results demonstrate that surface modification of PEEK enhances cell viability especially when comparing PP samples to PEP samples. On the third day, the samples

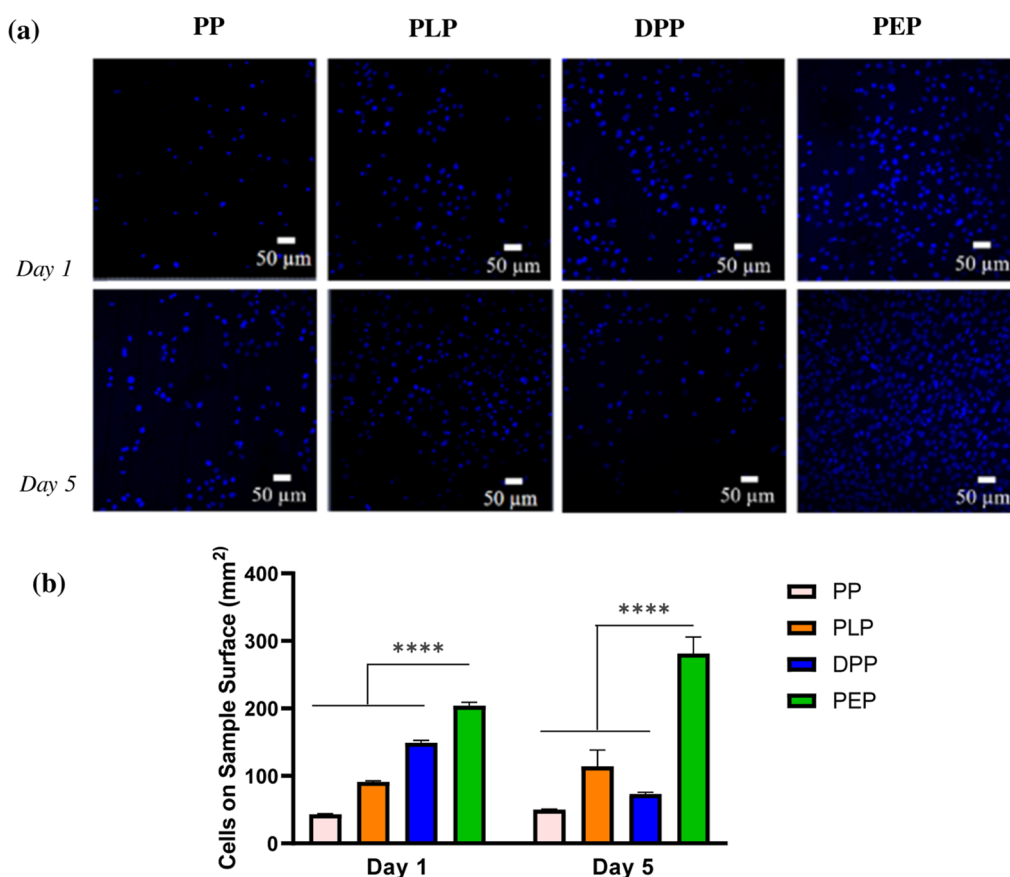


**Figure 7.** Fibroblast NIH/3T3 cell proliferation analyzing at days 1 and 5 for PP, PLP, DPP, and PEP samples and represented by (a) cell nucleus stained with Hoechst, (b) quantification using Image J software, ( $n = 2$  and 20 images per sample); \*\*\*\* represents  $p < 0.0001$  as compared to the PEP group.

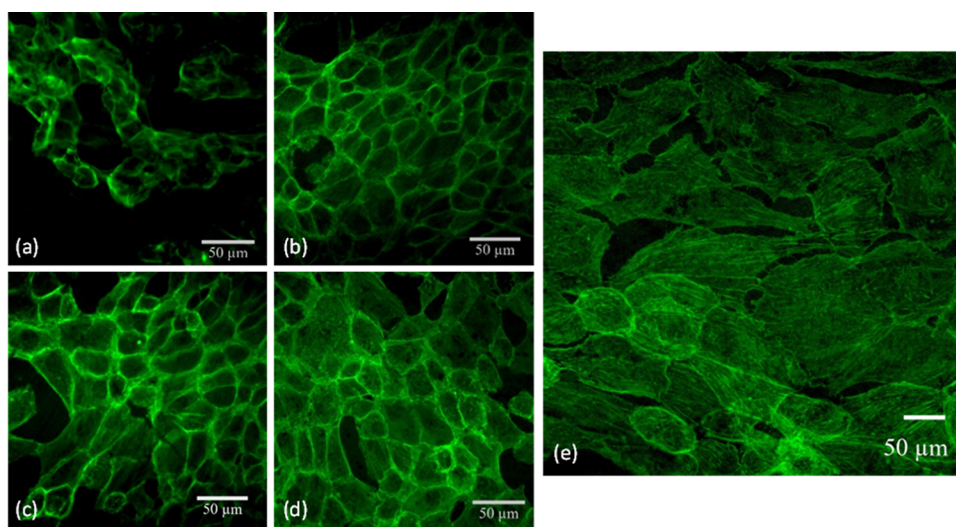


**Figure 8.** Fibroblast NIH/3T3 cells cultured on different PEEK surfaces, (a) PP, (b) PLP, (c) DPP, and (d) PEP after 1 day; and (e) PEP cells after 5 days. The images were taken in areas of significant cell confluence; the Cell cytoskeletons were stained with phalloidin. The nuclei were not shown here.

maintained an increasing viability like the first day without a notable increase specifically by the PEP sample. A possible explanation for this behavior could be some peptides detached from the surface, and the RGD sequence in solution favored the cell detachment.<sup>14</sup> On the fifth day, the viability increased in all samples except for the PLP that maintained a similar

viability percentage as the PLP sample on day 3. The DPP sample reached an acceptable viability of 83% ( $\pm 1.74$ ), while the PEP sample had an outstanding 96% ( $\pm 2.41$ ), suggesting that RGD peptide signaling was carried out on the trans-membrane integrin of the fibroblast cells. In general, it can be concluded the biofunctionalization with the peptide on PEEK

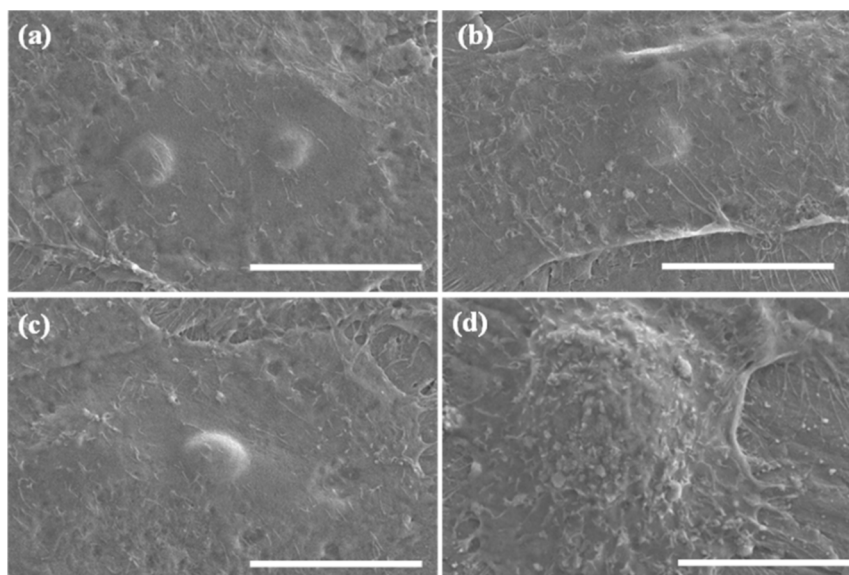


**Figure 9.** SEM fibroblast NIH/3T3 morphology after 8 h cultured on different PEEK surfaces, (a) PLP, (b) DPP, and (c) PEP. Image (d) represents the cell morphology encountered in some areas of DPP and PEP samples. Scale bars are 10  $\mu\text{m}$ .

surfaces (PEP) increases cell viability as opposed to the non-treated samples (PP).

**3.6.2. Cell Proliferation.** Proliferation analysis in the first and fifth day (top and bottom, respectively) are shown in Figure 7. Surface modification of PEEK samples increased the proliferation rate with time, and the results were related with MTT assays at the first and fifth day. The DPP sample for day 5 was the only sample that did not follow the increasing trend which is discussed later. Considering each PEEK-modified surface and the changes in surface chemistry and hydrophilicity, each modification impacted cell proliferation in a different way. Not surprisingly, the PP sample had a low cellular response due to the lack of surface functionalization. The plasma treatment (PLP) had a better effect on wettability and thus a greater number of cells compared to PEEK that was only polished. The changes in surface chemistry and hydrophilicity from the PDA coating on the DPP sample had favorable results on day 1 of exposure, however on day 5, cell proliferation was reduced in comparison to day 1. This result deviated from the trend seen in the viability assay at the same time of exposure. One probable explanation for this result, mentioned in other study as well, is the optical density of cells is not always linear.<sup>25</sup> One example in Yu ben lee et al., PDA coating on PCL films consistently showed low cell proliferation between days 3 and 14.<sup>13</sup> It may be possible that over time, coating with PDA alone does not maintain cell proliferation, however, to be sure of this more experimentation is needed, but it is beyond the scope of this paper. Finally, the sample with the RGD peptide had, by far, the highest cellular response at both test times, demonstrating that the peptide promotes an exceptional cell proliferation.

**3.6.3. Cell Adhesion and Spreading.** The cell adhesion and spreading are shown in Figure 8 where only the cytoskeleton was stained. Similar morphologies were observed especially on PLP, DPP, and PEP samples. As seen in Figure 8a, there does not appear to be a lot of spreading when compared to the other samples. In the other three samples, the cells have a more flattened appearance. Also in all samples, the cells were grouped into single areas. The cytoskeleton of the cells on the PEP samples from day 5 is more spread over the surface

compared to day 1 (Figure 8,e,d, respectively), affirming the PEEK modified with the RGD peptide provides a better anchor for cell adhesion.

Moreover, cells were cultured for 8 h and observed by SEM represented in Figure 9. The SEM images showed cells successfully anchored and spread in a similar manner on the different PEEK surfaces, as seen in Figure 9a–c. DPP and PEP samples also exhibited few cells with prominent nucleus and with observable residues most likely from the polymerization and peptide biofunctionalization confirmed in Figure 9d. The results here suggest the residues seen after polymerization and peptide biofunctionalization of PEEK samples aided cell adherence as well as morphology. About the PP sample, not attached cells were observed at this time.

## 4. CONCLUSIONS

Four different surface modifications to PEEK were performed and evaluated for their ability to interact with a biological microenvironment. A sequential modification with a polished surface (PP), oxygen plasma activation (PLP), PDA coating (DPP), and peptide functionalization (PEP) was accomplished to investigate the impact of these treatments on cellular response. The contact angle test showed increased wettability (hydrophilicity) as different treatments were completed. The chemical surface analysis by XPS revealed evidence of chemical elements, indicating that PDA coating and peptide functionalization were successful. This surface functionalization was confirmed by XRD analysis, where a phase attributable to the peptide was detected. Furthermore, the amount of peptide remaining over the surface was quantified through a semi-quantitative UV–vis analysis of the peptide concentration in solutions before and after surface functionalization. The *in vitro* studies established that the RGD peptide improved cellular bioactivity regarding adhesion, spreading, viability, and proliferation, enhancing the number of proliferated cells with each added surface modification. The PLP sample had an increased cell viability and proliferation rate concerning the PP control, indicating that plasma is a simple and effective treatment. The DPP sample with PDA showed a non-linear

cellular behavior with good viability results but not in proliferation. The outcomes specified that functionalized PEEK surface with RGD peptide significantly improves cellular interaction, demonstrated by high cell viability and proliferation in all time points tested and facilitating cellular adhesion and spreadability. The improved cellular response on the PEEK surface will undoubtedly make it a more biocompatible and bioactive biomaterial when implanted in the human body.

In brief, the methodology proposed in this work has demonstrated, according to the results and evidence, that it is possible to functionalize the PEEK surface with peptides through plasma treatment and surface chemistry. XPS, SEM, XRD, and UV–vis provided strong evidence of peptide attachment to the surface, which was challenging due to its close-packed semi-crystalline structure and unreactive surface. On the other hand, the in vitro studies with cellular cultures demonstrated that the very inert PEEK could be dramatically transformed into a bioactive polymer that promotes cell adhesion and spreading on its surface, making it a much better biocompatible and bioactive biomaterial. The bioactivated PEEK can be an improved biomaterial to fabricate biomedical implants and artificial body part replacement with better biocompatibility and cellular response. In addition, the methodology developed in this paper could be applied for surface functionalization of other biocompatible, inert polymers such as polyethylene or PMMA, among others, in order to increase their bioactive properties when implanted in the human body.

## AUTHOR INFORMATION

### Corresponding Author

Javier S. Castro – Universidad Autónoma de Ciudad Juárez, Ciudad Juárez 32310, Mexico; [orcid.org/0000-0002-4753-5606](https://orcid.org/0000-0002-4753-5606); Email: [jcastro@uacj.mx](mailto:jcastro@uacj.mx)

### Authors

Lillian V. Tapia-Lopez – Universidad Autónoma de Ciudad Juárez, Ciudad Juárez 32310, Mexico; Department of Pharmaceutical Sciences, University of Texas at El Paso, El Paso, Texas 79902, United States; [orcid.org/0000-0003-1279-0858](https://orcid.org/0000-0003-1279-0858)

María A. Luna-Velasco – Centro de Investigación en Materiales Avanzados, Chihuahua 31136, Mexico

Elfa K. Beaven – Department of Biomedical Engineering, College of Engineering, University of Texas at El Paso, El Paso, Texas 79968, United States

Alain S. Conejo-Dávila – Centro de Investigación en Materiales Avanzados, Chihuahua 31136, Mexico

Md Nurunnabi – Department of Pharmaceutical Sciences, University of Texas at El Paso, El Paso, Texas 79902, United States; Department of Biomedical Engineering, College of Engineering, University of Texas at El Paso, El Paso, Texas 79968, United States; [orcid.org/0000-0003-4457-3401](https://orcid.org/0000-0003-4457-3401)

Complete contact information is available at:

<https://pubs.acs.org/10.1021/acsbiomaterials.3c00232>

### Notes

The authors declare no competing financial interest.

## ACKNOWLEDGMENTS

We thank CONACYT for awarding the postdoctoral fellowship to Lillian Vianey Tapia Lopez (CVU 333687) in 2021–2022. The authors would also like to thank the laboratory

technicians Luis Silva, Karla Campos, Monica Mendoza, Cesar Leyva, Daniel Lardizabal, and Claudia Ramírez for their support in the characterization part.

## REFERENCES

- (1) Thakur, A.; Kumar, A.; Kaya, S.; Marzouki, R.; Zhang, F.; Guo, L. Recent Advancements in Surface Modification, Characterization and Functionalization for Enhancing the Biocompatibility and Corrosion Resistance of Biomedical Implants. *Coatings* **2022**, *12*, 1459.
- (2) Ng, I. C.; Pawijit, P.; Tan, J.; Yu, H. Anatomy and Physiology for Biomaterials Research and Development. *Encycl. Biomater. Biomed. Eng.* **2019**, *1–3*, 225–236 Elsevier.
- (3) Poulsson, A. H. C.; Mitchell, S. A.; Davidson, M. R.; Johnstone, A. J.; Emmison, N.; Bradley, R. H. Attachment of Human Primary Osteoblast Cells to Modified Polyethylene Surfaces. *Langmuir* **2009**, *25*, 3718–3727.
- (4) Kwon, G.; Kim, H.; Gupta, K. C.; Kang, I. K. Enhanced Tissue Compatibility of Polyetheretherketone Disks by Dopamine-Mediated Protein Immobilization. *Macromol. Res.* **2018**, *26*, 128–138.
- (5) Luo, R.; Tang, L.; Wang, J.; Zhao, Y.; Tu, Q.; Weng, Y.; Shen, R.; Huang, N. Improved immobilization of biomolecules to quinone-rich polydopamine for efficient surface functionalization. *Colloids Surf., B* **2013**, *106*, 66–73.
- (6) Al-Azzam, N.; Alazzam, A. Micropatterning of Cells via Adjusting Surface Wettability Using Plasma Treatment and Graphene Oxide Deposition. *PLoS One* **2022**, *17*, No. e0269914.
- (7) Poulsson, A. H. C.; Eglin, D.; Geoff Richards, R. Surface Modification Techniques of PEEK, Including Plasma Surface Treatment. In *PEEK Biomaterials Handbook*, 2nd Edition; Elsevier, 2019; pp 179–201.
- (8) Panayotov, I. V.; Orti, V.; Cuisinier, F.; Yachouh, J. Polyetheretherketone (PEEK) for medical applications. *J. Mater. Sci.: Mater. Med.* **2016**, *27*, 118.
- (9) Järvinen, S.; Suojanen, J.; Kormi, E.; Wilkman, T.; Kiukkonen, A.; Leikola, J.; Stoor, P. The Use of Patient Specific Polyetheretherketone Implants for Reconstruction of Maxillofacial Deformities. *Journal of Cranio-Maxillofacial Surgery* **2019**, *47*, 1072–1076.
- (10) Kurtz, S. M.; Devine, J. N. PEEK Biomaterials in Trauma, Orthopedic, and Spinal Implants. *Biomaterials* **2007**, *28*, 4845–4869.
- (11) Teng, R.; Meng, Y.; Zhao, X.; Liu, J.; Ding, R.; Cheng, Y.; Zhang, Y.; Zhang, Y.; Pei, D.; Li, A. Combination of Polydopamine Coating and Plasma Pretreatment to Improve Bond Ability Between PEEK and Primary Teeth. *Front. Bioeng. Biotechnol.* **2021**, *8*, 630094.
- (12) Mehdizadeh Omrani, M.; Kumar, H.; Mohamed, M. G. A.; Golovin, K.; S Milani, A.; Hadjizadeh, A.; Kim, K.; Kim, K. Polyether Ether Ketone Surface Modification with Plasma and Gelatin for Enhancing Cell Attachment. *J. Biomed. Mater. Res., Part B* **2021**, *109*, 622–629.
- (13) Lee, Y. B.; Shin, Y. M.; Lee, J. h.; Jun, I.; Kang, J. K.; Park, J. C.; Shin, H. Polydopamine-mediated immobilization of multiple bioactive molecules for the development of functional vascular graft materials. *Biomaterials* **2012**, *33*, 8343–8352.
- (14) Yang, Z.; Liu, M.; Yang, Y.; Zheng, M.; Yang, Y.; Liu, X.; Tan, J. Biofunctionalization of Zirconia with Cell-Adhesion Peptides: Via Polydopamine Crosslinking for Soft Tissue Engineering: Effects on the Biological Behaviors of Human Gingival Fibroblasts and Oral Bacteria. *RSC Adv.* **2020**, *10*, 6200–6212.
- (15) Bellis, S. L. Advantages of RGD Peptides for Directing Cell Association with Biomaterials. *Biomaterials* **2011**, *32*, 4205–4210.
- (16) Liao, J.; Wu, S.; Li, K.; Fan, Y.; Dunne, N.; Li, X. Peptide-Modified Bone Repair Materials: Factors Influencing Osteogenic Activity. *J. Biomed. Mater. Res. A* **2019**, *107*, 1491–1512.
- (17) Rochford, E. T. J.; Poulsson, A. H. C.; Salavarieta Varela, J.; Lezuo, P.; Richards, R. G.; Moriarty, T. F. Bacterial Adhesion to Orthopaedic Implant Materials and a Novel Oxygen Plasma Modified PEEK Surface. *Colloids Surf., B* **2014**, *113*, 213–222.



(18) Jia, L.; Han, F.; Wang, H.; Zhu, C.; Guo, Q.; Li, J.; Zhao, Z.; Zhang, Q.; Zhu, X.; Li, B. Polydopamine-assisted surface modification for orthopaedic implants. *Journal of Orthopaedic Translation* **2019**, *17*, 82–95.

(19) Lakshminarayanan, R.; Madhavi, S.; Sim, C. P. C. Oxidative Polymerization of Dopamine: A High-Definition Multifunctional Coatings for Electrospun Nanofibers - An Overview. In *Dopamine - Health and Disease*; InTech, 2018. DOI: DOI: 10.5772/intechopen.81036.

(20) Kontziampasis, D.; Trantidou, T.; Regoutz, A.; Humphrey, E. J.; Carta, D.; Terracciano, C. M.; Prodromakis, T. Effects of Ar and O<sub>2</sub> Plasma Etching on Parylene C: Topography versus Surface Chemistry and the Impact on Cell Viability. *Plasma Processes Polym.* **2016**, *13*, 324–333.

(21) Luque-Agudo, V.; Hierro-Oliva, M.; Gallardo-Moreno, A. M.; González-Martín, M. L. Effect of Plasma Treatment on the Surface Properties of Polylactic Acid Films. *Polym. Test.* **2021**, *96*, 107097.

(22) della Vecchia, N. F.; Luchini, A.; Napolitano, A.; Derrico, G.; Vitiello, G.; Szekely, N.; Dischia, M.; Paduano, L. Tris Buffer Modulates Polydopamine Growth, Aggregation, and Paramagnetic Properties. *Langmuir* **2014**, *30*, 9811–9818.

(23) Luo, R.; Tang, L.; Zhong, S.; Yang, Z.; Wang, J.; Weng, Y.; Tu, Q.; Jiang, C.; Huang, N. In Vitro Investigation of Enhanced Hemocompatibility and Endothelial Cell Proliferation Associated with Quinone-Rich Polydopamine Coating. *ACS Appl. Mater. Interfaces* **2013**, *5*, 1704–1714.

(24) Liyanage, M. R.; Bakshi, K.; Volkin, D. B.; Middaugh, C. R. Ultraviolet Absorption Spectroscopy of Peptides. *Methods Mol. Biol.* **2014**, *1088*, 225–236.

(25) Ghasemi, M.; Turnbull, T.; Sebastian, S.; Kempson, I. The Mtt Assay: Utility, Limitations, Pitfalls, and Interpretation in Bulk and Single-Cell Analysis. *Int. J. Mol. Sci.* **2021**, *22*, 12827.

(26) Tapia-Lopez, L. V.; Esparza-Ponce, H. E.; Luna-Velasco, A.; Garcia-Casillas, P. E.; Castro-Carmona, H.; Castro, J. S. Bioactivation of Zirconia Surface with Laminin Protein Coating via Plasma Etching and Chemical Modification. *Surf. Coat. Technol.* **2020**, *402*, 126307.

(27) Doumeng, M.; Makhlof, L.; Berthet, F.; Marsan, O.; Delbé, K.; Denape, J.; Chabert, F. A Comparative Study of the Crystallinity of Polyetheretherketone by Using Density, DSC, XRD, and Raman Spectroscopy Techniques. *Polym. Test.* **2021**, *93*, 106878.

(28) Thanigachalam, M.; Muthusamy Subramanian, A. V. Evaluation of PEEK-TiO<sub>2</sub>-SiO<sub>2</sub> Nanocomposite as Biomedical Implants with Regard to in-Vitro Biocompatibility and Material Characterization. *J. Biomater. Sci., Polym. Ed.* **2022**, *33*, 727–746.

(29) Han, T. H.; Park, J. S.; Oh, J. K.; Kim, S. O. Morphology Control of One-Dimensional Peptide Nanostructures. *J. Nanosci. Nanotechnol.* **2008**, *8*, 5547–5550.

(30) Giri, R. S.; Mandal, B. Boc-Val-Val-OMe (A $\beta$ 39-40) and Boc-Ile-Ala-OMe (A $\beta$ 41-42) Crystallize in a Parallel  $\beta$ -Sheet Arrangement but Generate a Different Morphology. *CrystEngComm* **2018**, *20*, 4441–4448.